Expression of xeroderma pigmentosum complementation group C protein predicts cisplatin resistance in lung adenocarcinoma patients

TAN-CHEN LAI[1,2], KUAN-CHIH CHOW[3], HSIN-YUAN FANG[4], HSIN-CHING CHO[3]
CHIH-YI CHEN[4], TZE-YI LIN[5], I-PING CHIANG[5] and SHU-PENG HO[2]

[1]Department of Medical Laboratory Science and Biotechnology, Central Taiwan University of Science and Technology, Taichung; [2]Department of Veterinary and [3]Graduate Institute of Biomedical Sciences, National Chung Hsing University, Taichung; Departments of [4]Surgery and [5]Pathology, China Medical University Hospital, Taichung, Taiwan, R.O.C.

Received October 5, 2010; Accepted December 13, 2010

DOI: 10.3892/or.2011.1184

Abstract. DNA repair has been suggested to be a major cause of spontaneous drug resistance in patients with lung adenocarcinomas (LADC). Among the DNA repair-related proteins, excision repair cross-complementation group 1 (ERCC1) has been shown to be essential for repairing cisplatin-induced interstrand cross-linkage. However, the role of other DNA repair-related proteins in drug resistance has not been clearly elucidated. In this study, we used suppression subtractive hybridization and microarray analysis to identify the DNA repair-related genes associated with cisplatin resistance. We focused on the association of XPC protein expression, which plays a pivotal role in the earliest response to global genomic repair, with the survival of LADC patients. Using suppression subtractive hybridization and a microarray analysis to identify drug resistance-associated DNA repair-related genes, we found that the mRNA levels of ERCC1, MSH-3, MSH-6 and XPC were significantly increased in LADC patients. Since the results of ERCC1 mRNA expression corresponded well with those in previous reports, in this study we focused on the clinical correlation between XPC expression and patient survival. The level of XPC protein was determined by immunohistochemical and immunoblotting analyses. We detected the XPC protein in 46 (43%) of 107 pathological LADC samples. XPC protein expression correlated with tumor stage, cigarette smoking and poor survival. In the *in vitro* experiments with LADC cell lines, increased XPC expression was associated with elevated drug resistance, and silencing of XPC expression reduced cisplatin resistance. Our results suggest that XPC expression predicts drug resistance in LADC.

Correspondence to: Dr Kuan-Chih Chow, Graduate Institute of Biomedical Sciences, National Chung Hsing University, Taichung, Taiwan, R.O.C.
E-mail: kcchow@dragon.nchu.edu.tw

Dr Shu-Peng Ho, Department of Veterinary Medicine, National Chung Hsing University, Taichung, Taiwan, R.O.C.
E-mail: spho@dragon.nchu.edu.tw

Abbreviations: DRR, DNA repair-related; ERCC1, excision repair cross-complementation group 1; hHR23, human homolog of yeast Rad23 protein; LADC, lung adenocarcinoma; MSH, mutS homolog; NER, nucleotide excision repair; NSCLC, non-small cell lung cancer; NTLT, non-tumor lung tissues; PKC, protein kinase C; UV, ultraviolet; UVRAG, UV radiation resistance associated gene; XPC, xeroderma pigmentosum complementation group C; XPF, xeroderma pigmentosum complementation group F; XRCC, X-ray repair cross complementing group

Key words: XPC, nucleotide excision repair, cisplatin resistance, lung adenocarcinoma

Introduction

Lung cancer is one of the leading causes of cancer-related death worldwide. Based on the presence of neuroendocrine features, lung carcinomas are categorized into small cell lung cancer (SCLC) and non-small cell lung cancer (NSCLC) (1). Moreover, depending on the histopathological characterization, NSCLC is subcategorized into lung adenocarcinoma (LADC), squamous cell carcinoma and large cell carcinoma (2). Among these, LADC is featured by rapid growth, high metastatic potential and high frequency of spontaneous resistance to anticancer drugs as well as radiation therapy, all of which indicate a poor prognosis (2).

Accumulating evidence has shown that tobacco, and particularly its constituents, e.g., polycyclic aromatic hydrocarbon (PAH) compounds, induce DNA damage and may therefore activate DNA repair system prior to chemo- or radiotherapy (3-5). Niedernhofer *et al* found that excision repair cross-complementation group 1 (ERCC1) and xeroderma pigmentosum complementation group (XP) F were required for repairing cisplatin-induced interstrand cross-linkage and suggested that DNA repair was involved in drug resistance (6). Olaussen *et al* found that clinically, NSCLC patients with ERCC1-negative tumors responded better to cisplatin-based adjuvant chemotherapy than those with ERCC1-positive

tumors did and hence the prognosis was better in the former. In contrast, patients with ERCC1-positive tumors survived longer than patients with ERCC1-negative tumors when adjuvant chemotherapy was not included in the regimens (7). These results suggest that ERCC1 expression may be associated with not only increased drug resistance, but also tumor metastatic potential, which is indicated by rapid tumor recurrence and distal organ dissemination. However, the role of the other DNA repair-related proteins in drug resistance is not clear.

To better understand the involvement of the DNA repair mechanism in drug resistance (8-11), specific genes related to this phenomenon must be identified. In this study, we combined suppression subtractive hybridization (SSH) and oligonucleotide microarray to compare the expression profiles of DNA repair-related (DRR) genes between LADC specimens from patients who responded well to cisplatin treatment and those who had early recurrence or distal metastasis following the equivalent therapy. We verified the results using reverse transcription-polymerase chain reaction (RT-PCR), and determined DRR protein localization in the pathological sample by immunohistochemical analysis. We also statistically evaluated the correlations of clinicopathological parameters and prognostic significance with DRR gene expression in LADC patients. Furthermore, using *in vitro* experiments with LADC cell lines, we determined the effects of tobacco and nicotine on DRR gene expression and the effects of DRR gene expression on cisplatin resistance.

Materials and methods

Patients and tissue specimens. The patients in this study were from the same cohort as that in our previous study (4). The Medical Ethics Committee of China Medical University Hospital approved the study protocol, and every patient provided written informed consent before surgery. Briefly, from January to December 2001, tissue specimens were collected from 107 patients with newly diagnosed LADC. LADC was confirmed by pathological examination of the samples from all patients for whom at least one follow-up examination or death was documented. The stage of the disease was classified according to the new international staging system for lung cancer (12). All patients had undergone surgical resection and radical N2 lymph node dissection. Tumor size, number of affected lymph node, differentiation, vascular invasion and mitotic number were also evaluated. Patients with lymph node involvement or loco-regional recurrence received irradiation at the afflicted areas. Those with distant metastasis were treated with chemotherapy. After treatment, the patients were routinely followed up every 3-6 months in the outpatient department. The results of blood examination, biochemical studies, chest radiography scans, abdominal sonography scans, whole body bone scans, and chest computerized tomography scans that indicated any evidence of disease were interpreted as tumor recurrence and metastasis. The average age of the male patients (n=62) was 60.6±1.41 years and that of the female patients (n=15) was 53.3±1.27 years (p=0.0154). Immunohistochemical staining was carried out using a single-blind procedure.

RNA extraction, suppression subtractive hybridization and microarray. Total RNA was isolated from frozen tissues by using a SNAP RNA column (Invitrogen, San Diego, CA). After the RNA yield was measured, cDNA primed with oligo random primers was synthesized by AMV reverse transcriptase. The combined SSH and microarray method was as described previously (4,13). Briefly, following the synthesis of first-strand cDNA with random primers and AMV reverse transcriptase, second-strand cDNA was synthesized using T4 DNA polymerase to form double-stranded DNA. An equal amount of cDNA from 10 patients, who had early recurrence or distal metastasis following cisplatin-based therapies, was pooled (labeled as 'non-responder') and digested with the restriction enzyme *Rsa*I. The reaction product was then ligated to 2 specific adaptors (tagged-pool, refer to instruction manual of BD Biosciences, at http://www.bdbiosciences.com/clontech). After forward SSH was performed against a cDNA pool synthesized from non-tumor lung tissue counterparts to exclude genes that were concomitantly expressed in both tumor and non-tumor lung, the reaction mixtures were subjected to 35 cycles of PCR using the standard procedure: denaturation at 94˚C for 45 sec, hybridization at 56˚C for 30 sec, and elongation at 72˚C for 45 sec. The amplified products were resolved in a 2.5% agarose gel, and visualized by ethidium bromide staining to determine the efficacy of SSH. For reverse SSH, cDNA from 10 lung cancer tissues collected from patients who had responded well to cisplatin treatment was used as a tagged-pool (labeled as responder) to hybridize against cDNA from non-responder lung cancer samples.

The resultant SSH cDNA libraries were then labeled with the respective fluorescent nucleotides, and the reaction mixture was hybridized to microarray slides (Taiwan Genome Sciences, Taipei, Taiwan) to identify the corresponding gene(s). The microarray test was performed in triplicate, and each corresponding gene was mapped out. The ratio between the normalized fluorescent signal intensities of the genes in the responder lung cancer tissues and non-responder tumor tissues was measured on individual spots in the microarray, and the values of the 3 readings were averaged. The cut-off ratio for strongly expressed genes was set at 2.0 (with 99.5% coefficient variance in a scatter plot), and that for down-regulated genes was set at 0.5. If the expression ratio fell between 0.5 and 2.0, the gene was considered constitutive.

RT-PCR. Following total RNA extraction and synthesis of first-strand cDNA, an aliquot of cDNA was subjected to 35 cycles of PCR using primers for ß-actin to determine the integrity of mRNA pool (4,5). The cDNA used in the following RT-PCR was adjusted according to the quality and quantity of ß-actin mRNA. Primer3 (http://frodo.wi.mit.edu/primer3) was used to select the primer sequences. The primers for XPC are as follows: 5'-GAAGAAAGAAGAC TTGGAG-3' (XPCs; sense primer, nts 1958-1976, NM_004628) and 5'-GCTCACAGCTGCTCAAATGG-3' (XPCa; antisense primer, nts 2929-2910). The primers for ß-actin are as follows: 5'-AGAGCTACGAGCTGCCTGAC-3' (sense primer, nts 797-816, NM_001101.3) and 5'-CACTT CACCGTTCCAGTTT-3' (antisense primer, nts 1375-1356). The size of the amplified DNA fragment for XPC is 972 bp and for ß-actin is 579 bp.

Cytotoxicity assay. At 18 h before challenge with cisplatin at various concentrations, 5000 cells/well were seeded. Control cells were treated with RPMI-1640. After cell challenge for 48 h, 10 μl of WST-1 (BioVision, Mountain View, CA) was added to the cell culture, and incubation was continued for 2 h. The percentage of surviving cells was quantified by comparing the number of viable cells in the treatment group with that in the control group. All procedures were performed in triplicate. This assay measures both replicating and static cells (4,5).

Preparation of mouse antibodies. The DNA sequence corresponding to C-terminal fragment (amino acid residues 618-940) of human XPC (hXPC-C) was amplified using primer sequences containing *Eco*RI (sense) and *Hin*dIII (antisense) restriction sites. The primer sequences were 5'-TCCGAATTCATGGAAGAAAGAAGACTTGGAG-3' (*XPCs*; the *Eco*RI site is underlined) and 5'-GCAAGCTTGGCTCACAGCTGCTCAAATGG-3' (*XPCa*; the *Hin*dIII site is underlined).

The restriction fragment of hXPC was cloned into the expression vector pET-32b$^+$ (Promega KK, Tokyo, Japan). Bacterial colonies containing pET32+ -hXPC-C were selected and were induced using isopropyl-beta-D-thio-galactopyranoside (IPTG) to mass-produce hXPC-C. The recombinant protein was purified using a nickel-affinity column. Affinity-purified hXPC-C was used to immunize BALB/c mice, and the sensitivity of the antiserum (OD405 >0.3 at 1:6000 dilutions) was measured by enzyme-linked immunosorbent assay (ELISA). The specificity of the antibodies was determined by the appearance of a 125-kDa band in the immunoblotting test with lung cancer cell extract (14). Monoclonal antibodies were produced by the hybridoma technique, and XPC-specific antibodies were screened by the above-mentioned methods.

Immunoblotting analysis. Total cell lysate was prepared by mixing 5x10^7 cells/100 μl phosphate-buffered saline with an equal volume of 2X loading buffer [50 mM Tris (pH 6.8), 150 mM NaCl, 1 mM disodium EDTA, 1 mM PMSF, 10% glycerol, 5% ß-mercaptoethanol, 0.01% bromophenol blue and 1% SDS]. Electrophoresis was carried out in a 10% polyacrylamide gel with 4.5% stacking gel. After electrophoresis, the proteins were transferred to a nitrocellulose membrane for immunoblotting. The membrane was probed with specific antibodies. The signal was amplified using biotin-labeled goat anti-mouse IgG, and peroxidase-conjugated streptavidin. The protein was visualized by exposing the membrane to an X-Omat film (Eastman Kodak, Rochester, NY) with enhanced chemiluminescent reagent (NEN, Boston, MA).

Immunocytochemical and immunohistochemical analysis. Immunocytochemical and immunohistochemical staining was performed using the immunoperoxidase method with labeled streptavidin-biotin complex (Dako, LSAB2 System, Carpenteria, CA) (4,5). For confocal immunofluorescence microscopy, secondary antibodies tagged with fluorescence proteins were used. Briefly, following the removal of paraffin with xylene and absolute alcohol, the antigen was retrieved by boiling the samples in water for 10 min. Endogenous myeloperoxidase was inactivated with 3% H_2O_2 and 0.1% sodium azide at room temperature for 15 min. After incubation with monoclonal antibodies (1:100 dilutions) specific to XPC at room temperature for 2 h, the specimens were treated with biotin-conjugated goat anti-mouse immunoglobulin and then peroxidase-conjugated streptavidin. 3-amino-9-ethylcarbazole (AEC) was used for chromogenic development. The slides were counterstained with 50% hematoxylin in tap water at room temperature for 45 sec and the blue color was enhanced in running water for 20 min. The presence of crimson precipitates was considered as positive staining. A section of gelatin-embedded H23 LADC cells was used as the positive control and that of non-tumor lung tissue (NTLT) cells served as the negative control for each run of immunostaining.

Knockdown of XPC expression using the RNAi method. Human embryonic kidney 293T cells were cultured in DMEM with 10% fetal serum until ~50-70% confluence. The cells were transfected with a mixture of packaging plasmid (pCMV-ΔR8.91, containing the *gag*, *pol* and *rev* genes), envelope plasmid (pMD.G, a VSV-G-expressing plasmid) and plasmid containing pLKO.XPC1-shRNA. Lentivirus containing pLKO.XPC1-shRNA was harvested on days 3 and 4 post-transfection. LADC H23 cells were infected with lentivirus containing XPC1-shRNA, and the infected cells were selected using puromycin. Knockdown of XPC expression was assayed using an immunoblotting method.

Slide evaluation. For each pathological section, NTLT served as the internal negative control. Slides were evaluated by 2 pathologists who were blinded to the clinicopathological details. The ImmunoReactive Scoring system was adapted in this study (15). Briefly, the signals in a specimen were considered as strong when >50% of the cancer cells were positively stained, intermediate when 25-50% of the cells were positively stained, weak when <25% or >10% of the cells were positively stained, and negative if <10% of the cells were positively stained. Cases with strong and intermediate XPC signals were classified as XPC$^+$, and those with weak or negative XPC signals were classified as XPC$^-$.

Statistical analysis. The relationship between XPC expression and clinicopathological parameters was analyzed using the χ^2 test. Survival curves were plotted using the Kaplan-Meier estimator (16). The statistical difference in the survival between different groups was compared by the log-rank test (17,18). Statistical analysis was performed using the GraphPad Prism5 statistical software (San Diego, CA). Statistical significance was set at p-value <0.05.

Results

Expression panels of DRR genes in cisplatin-resistant LADC. By combining SSH (Fig. 1A) and oligonucleotide microarray (Fig. 1B) to compare the gene expression patterns between pooled tumor fractions from 10 LADC patients who had early recurrence or distal metastasis following cisplatin-based adjuvant chemotherapies and those who responded well to the cisplatin regimens, we identified the differential

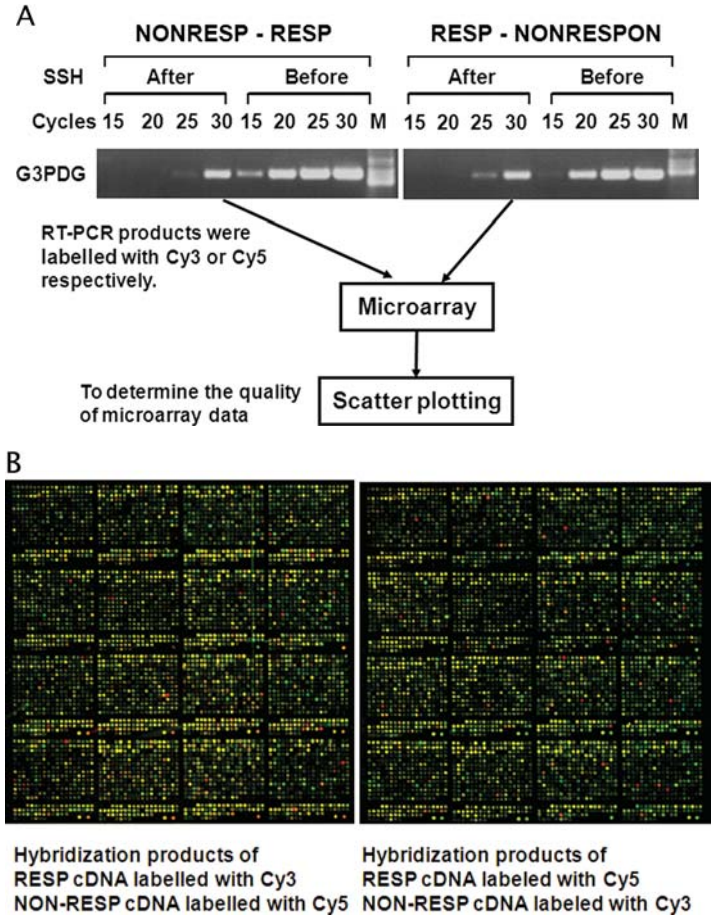

Figure 1. Representative image of suppression subtractive hybridization (SSH) and a microarray for comparing gene expression patterns between LADC tumors from patients who did not respond well (non-responder, NONRESP) and those who responded well (responder, RESP) to cisplatin therapy. (A) Following reverse transcription of polyA RNA cDNA, products from either non-responder or responder were divided and ligated to 2 different adaptors (to yield tester cDNA). Tester cDNA was hybridized to driver cDNA (cDNA without adaptors) to exclude commonly expressed gene sequences. The hybridization product was amplified by PCR to enrich differentially expressed sequences. The RT-PCR products were individually labeled with fluorescent dye Cy3 (red) or Cy5 (green), and hybridized to oligonucleotide microarray slides. The hybridized microarray slides were scanned, and the data were analyzed using a scatter plot program to determine the quality of the microarray results. (B) Representative results of microarray data.

Table I. Three different expression panels of DNA repair-related genes in advanced stage of LADC.

Up-regulated	Constitutive expressed	Down-regulated
ERCC-1 (3.57)[a]	ERCC2 (0.91)	UVRAG (0.36)
MSH3 (2.36)	ERCC4 (XPF) (0.70)	
MSH6 (4.32)	ERCC5 (0.64)	
XPC (2.089)	MSH2 (1.05)	
	MSH4 (0.88)	
	MSH5 (1.20)	
	p53 (1.13)	
	XPA (1.23)	
	XPB (0.63)	
	XPG (1.61)	
	XRCC3 (0.56)	

[a]Ratio between fluorescent signal intensities in lung cancer and non-tumor counterparts measured on individual spots of microarray. The values presented in parenthesis are the average readings of 3 spots on the microarray. The cut-off ratio for up-regulated gene was set at 2.0 (with 99.5% of coefficient variance in a scatter plot), and that for down-regulated gene was set at 0.5. If the expression ratio of a gene that fell between 0.5 and 2.0, it was considered constitutive.

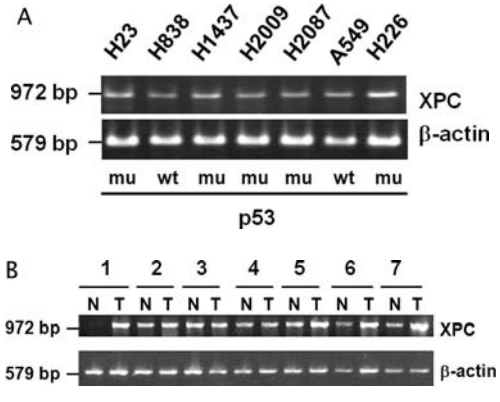

Figure 2. Expression of XPC mRNA detected by RT-PCR. Detection of XPC mRNA in (A) LADC cell lines and (B) LADC tissues by RT-PCR. Expression of ß-actin was used as a monitoring standard for the relative expression ratio of XPC mRNA. wt, wild-type p53; mu, mutant p53; T, LADC; N, non-tumor lung tissues.

expression spectra of DDR genes (Table I). The expression of ERCC-1, mutS homolog (MSH)-3, MSH-6 and XPC increased; that of ERCC2, ERCC-4 (also called XPF),

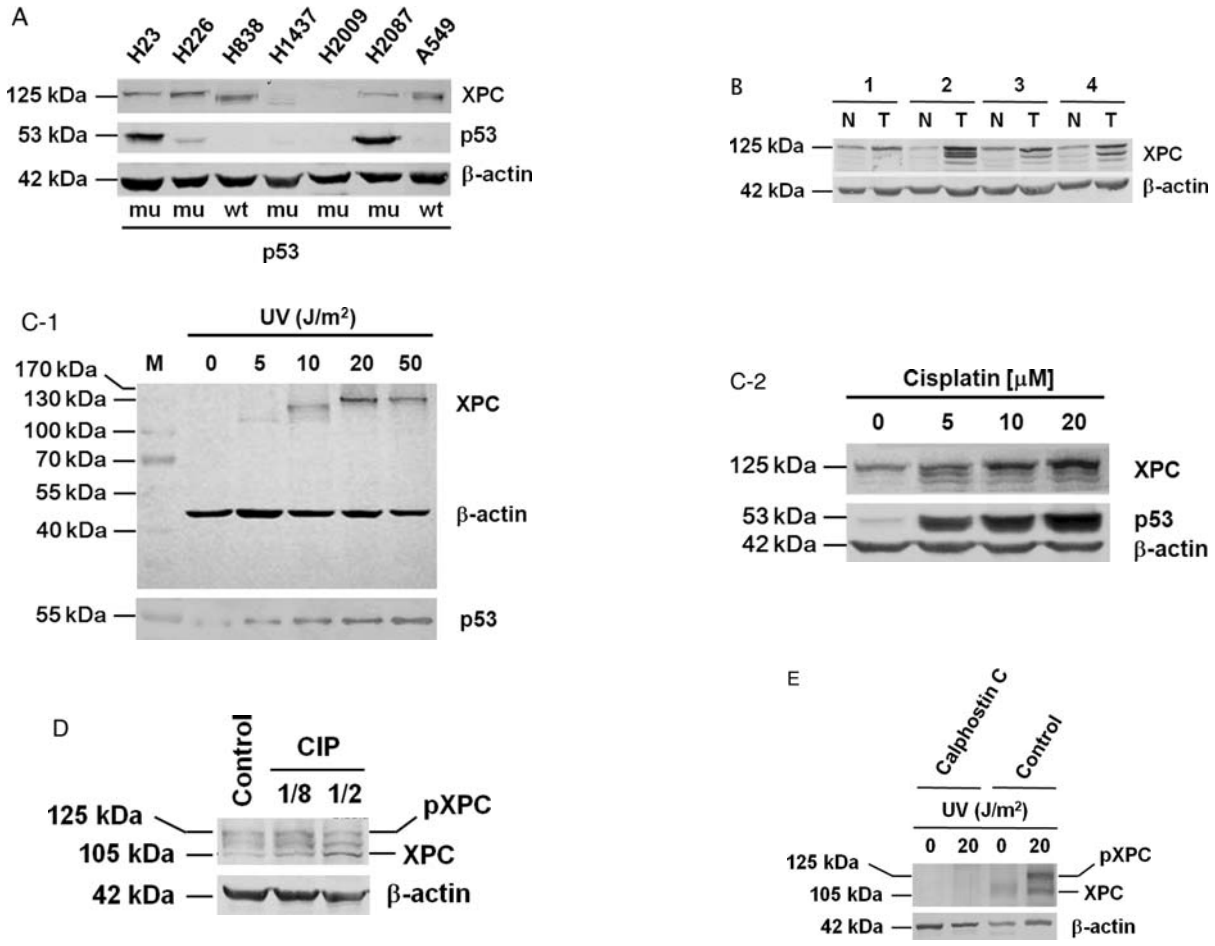

Figure 3. Characterization of monoclonal antibodies to XPC. (A) Using immunoblotting, the expression of 125-kDa XPC was detected in H23, H226 and H2087 cells. In H838, H1437 and A549 cells, however, a ladder of XPC signals was identified. wt, wild-type p53; mu, mutant p53. (B) The ladder of XPC signals was recognized in LADC specimens. (C) Because DNA damage caused by ultraviolet (UV) irradiation or cisplatin induces expression of XPC and p53, we (2C1) irradiated H1437 cells with UV (20 J/m^2) or (2C2) treated H226 cells with cisplatin at various concentration for 1 h in order to confirm the specificity of antibodies. The cells were then incubated at 37˚C for 1 h before immunoblotting. The monoclonal antibodies recognized the increased amount of p53 and the protein ladder as well as the expected 125-kDa XPC. (D) A549 Cell lysate was treated with calf intestinal alkaline phosphatase (CIP) before immunoblotting; the 125-kDa protein band was less intense, while the 105-kDa protein band was more intense. (E) Addition of 5 μM calphostin C, a pan-protein kinase C (PKC) inhibitor, to H1437 cells at 37˚C for 2 h before UV irradiation reduced UV-induced expression of 125-kDa XPC, suggesting that XPC phosphorylation is essential for maintaining protein stability. Moreover, because several bands were detected in the immunoblots, the results suggested that the number of XPC phosphorylation sites could be higher than that predicted by the web programs [NetPhos program (http://www.cbs.dtu.dk/services/NetPhos/) to predict phosphorylation sites, and NetPhosK program (http://www.cbs.dtu.dk/services/NetPhosK/) to predict specific kinase in eukaryotic proteins]. (F) Immunocytochemical examination of XPC expression in A549 cells. XPC was abundantly present in the cytoplasm and nucleolus (left panel). After UV irradiation, the XPC signals were mainly detected in the nucleus (right panel), and those on nucleoli reduced.

ERCC5, MSH-2, MSH-4, MSH-5, p53, XPA, XPB, XPG, X-ray repair cross complementing group (XRCC)-1, and XRCC-3 did not change; and that of ultraviolet radiation resistance associated gene (UVRAG) decreased. We then focused on XPC expression.

Expression of XPC in LADC cells determined by RT-PCR. The expression of XPC mRNA was determined by RT-PCR in 7 pairs of lung cancer biopsies. Interestingly, XPC overexpression was detected in 4 cancer specimens (Fig. 2A). Sequence analysis [by Mission Biotech, Taipei, Taiwan, on ABI PRISM model 3730 (www.missionbio.com.tw)] showed that the nucleotide sequences of cDNA fragments from the 4 LADC biopsies matched the nucleotide sequence of XPC: xeroderma pigmentosum, complementation group C (XPC), *Homo sapiens*, NM_004628, mRNA, identities = 969/972 (99.5%). XPC mRNA expression in 7 lung cancer cell lines that either carried wild-type or mutant *p53* gene was also determined by RT-PCR (Fig. 2B), and it was detected in all 7 cell lines. Likewise, the nucleotide sequences of the cDNA fragments matched the sequence of XPC. Further, 4 point mutations were identified: 109CTA→109GTA (Glu34Asp) was found in 5 of the 7 samples; 544AAG→544ATG (Lys180Met) in 3 of the 7 samples; 616GGG→616GGC (silent) in 1 of the 7 samples; and 1273CGG→1273CCG (Arg423Pro) in all 7

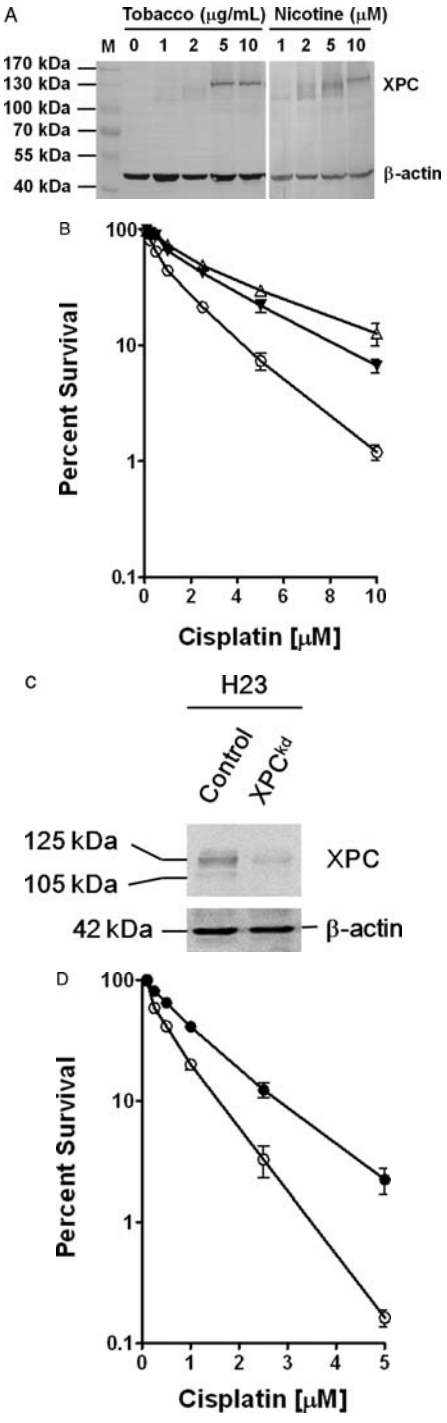

Figure 4. Effect of XPC expression on cisplatin cytotoxicity. (A) Addition of tobacco solution or nicotine at 37˚C for 4 h induced XPC expression. (B) Increase in XPC expression reduced cisplatin sensitivity. ○, control H1437 cells; ▼, H1437 cells treated with 10 μM of nicotine prior to cisplatin treatment; Δ, H1437 cells treated with 10 μg/ml of tobacco solution prior to cisplatin treatment, (C) RNAi reduced about 85% of the XPC expression in H23 cells [knockdown XPC (XPC^{kd})-specific expression]. (D) Compared to the control H23 cells (●), XPC^{kd} cells (○) were significantly more sensitive to cisplatin.

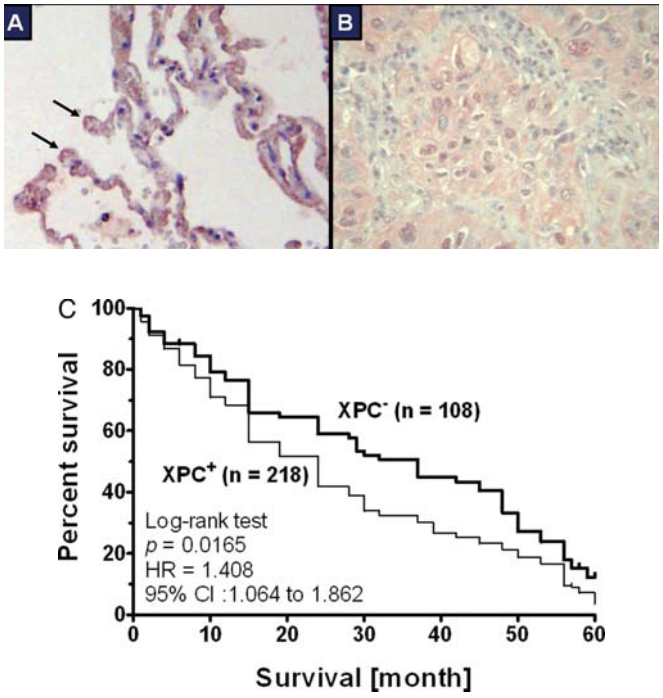

Figure 5. Correlation between XPC expression and survival of LADC patients. Representative examples of XPC expression in pathological specimens as detected by immunohistochemical staining (crimson precipitates). XPC was detected in (A) type II pneumocytes and in (B) LADC cells. (C) Comparison of Kaplan-Meier product limit estimates of survival analysis in LADC patients. Patients were divided into 2 groups depending on the expression of XPC. The difference in survival between the 2 groups was compared by the log-rank test (p=0.0214).

samples (the sequences were added to GenBank: HM113488). However, none of these mutations is equivalent to those found in patients with xeroderma pigmentosum (14).

Characterization of monoclonal antibodies to XPC and expression of XPC in LADC cell lines. Specificity of the monoclonal antibodies was determined by immunoblotting analysis with H23 cell lysate, wherein we recognized a 125-kDa protein band, which was ~20-kDa larger than the expected molecular mass of XPC (105-kDa) (Fig. 3A). We identified a ladder of XPC signals in other cell lines, i.e., H226, H838, H1437 and A549 (Fig. 3A). Interestingly, we also found this ladder of XPC signals in the cases of the lung cancer specimens (Fig. 3B). The results corresponded well with those presented in a report by Fautrel *et al* that XPC appeared in ladder forms in pathological samples of hepatocellular carcinomas (19). Moreover, a study by Adimoolam and Ford showed that levels of XPC and p53 increased following UV irradiation (20). To confirm the specificity of our antibodies, we irradiated H1437 cells with UV (20 J/m2) (Fig. 3C1) or treated H226 cells with cisplatin at various concentrations (Fig. 3C2), and the monoclonal antibodies recognized the protein ladder with the increased molecular mass of XPC and the 125-kDa XPC protein band in the immunoblots.

It is worth noting that cisplatin treatment increased p53 expression (Fig. 3C2). When cell lysates were treated with calf intestinal alkaline phosphatase (CIP) before immunoblotting, the amount of the 125-kDa protein was reduced, but that of the 105-kDa protein was increased (Fig. 3D). These results suggest that the 125-kDa XPC could be a phosphorylated form. UV irradiation and cisplatin treatment could induce XPC phosphorylation and stabilization. The NetPhos program (http://www.cbs.dtu.dk/services/NetPhos/) was used to predict phosphorylation sites and the NetPhosK program

Table II. Correlation of XPC expression with clinicopathological parameters in LADC patients.

Parameter	Expression of XPC		P-value	
	High (n=46)	Low (n=61)	Univariate	Multivariate
Gender				
Male (n=84)	40	44	0.065[a]	
Female (n=23)	6	17		
Cigarette smoking[b]				
Smoker (n=62)	40	22	<0.001[c]	0.002
Non-smoker (n=45)	6	39		
Stage				
I (n=26)	4	22	0.002[c]	0.029
II (n=31)	19	12		
III (n=50)	23	27		
Cell differentiation				
Well (n=17)	7	10	0.394[a]	
Moderate (n=60)	23	37		
Poor (n=30)	16	14		
Lymphovascular invasion				
Positive (n=81)	39	42	0.057[a]	
Negative (n=26)	7	19		

[a]Two-sided p-value determined by χ^2 test. [b]In this study, a smoker is defined as a person who smokes >1 pack per week (~50 packs/year). [c]Two-sided p-value determined by Fisher's exact test.

(http://www.cbs.dtu.dk/services/NetPhosK/) to predict the presence of specific kinases among eukaryotic proteins. The results showed that the most probable kinase was protein kinase C (PKC), and the putative phosphorylation sites were ^{79}Thr, ^{507}Ser and ^{711}Ser. Addition of 5 μM calphostin C (21), a PKC inhibitor, reduced the extent of the DNA damage-induced increase in 125-kDa XPC (Fig. 3E), indicating that phosphorylation was essential for maintaining XPC protein stability. Moreover, because 3 bands were detected in the immunoblots, the 3 phosphorylation sites of XPC predicted by the web programs are accurate. Immunocytochemical analysis showed that XPC was abundantly present in the cytoplasm and nucleolus (Fig. 3F, left panel). After UV treatment, the XPC signals were mainly detected in the nucleus (Fig. 3F, right panel), and those in the nucleolus were reduced. These data suggested that DNA damage induced translocation of XPC to the nucleus.

Elevated expression of 125-kDa XPC increases cisplatin resistance. Addition of tobacco solution [tobacco from a cigarette containing 0.9 mg of nicotine (Marlboro, USA) was soaked in distilled water at room temperature for 15 min to yield 10 μg/ml tobacco solution] or nicotine to H1437 cells increased the level of 125-kDa XPC (Fig. 4A) and cisplatin resistance (Fig. 4B). Moreover, using RNAi to knockdown XPC (XPCkd)-specific expression in H23 cells (Fig. 4C) significantly reduced cisplatin resistance (Fig. 4D), supporting our hypothesis that XPC expression increased cisplatin resistance in cancer cells.

Expression of XPC in LADC. Immunohistochemical analysis demonstrated the presence of XPC in 46 (43.0%) of the LADC pathological samples. XPC was also detected in type II pneumocytes (Fig. 5A). In 41 (89.1%) of the pathological specimens, XPC was identified in the nuclei of cancer cells (Fig. 5B). XPC expression was also detected in 39.3% (22/56) of metastatic lymph nodes (data not shown). Statistical analysis showed that overexpression of XPC in tumors correlated with tumor stage and cigarette smoking but not with lymphovascular involvement (Table II), suggesting that XPC expression could be associated with growth of LADC cells. Moreover, among 46 patients with high levels of XPC, 29 (63.0%) had tumor recurrence during follow-up examination. On the other hand, among 61 patients with low levels of XPC, 13 had tumor recurrence (21.3%). All 42 patients with recurrence had developed tumors within 24 months of operation. The risk of recurrence for patients with high levels of XPC was 1.73-fold higher than that for patients with low levels of XPC (p=0.074). The survival of patients with low XPC levels was significantly better than that of patients with high XPC levels (Fig. 5C). The hazard ratio between these 2 groups was 1.707, and the difference in cumulative survival was significant (p=0.0214) when the 2 groups were compared by the log-rank test (17,18). Using multivariate analysis, which included variables such as gender, cigarette smoking, tumor stages, status of cell differentiation, lymphovascular invasion and XPC expression, the statistical difference in survival between these 2 patient groups, however, was not significant (p=0.132).

Discussion

Our results showed that the antibodies generated in this study recognized both functional XPC, which is normally present in the cytoplasm and nucleoli, and nuclear XPC, which is frequently detected in pathological sections of LADC and in UV-irradiated cells. Based on the results, we inferred that XPC expression is associated with cigarette smoking and, possibly, cigarette ingredient-related DNA damage as well as the disease progression of LADC.

As shown in the immunoblotting experiment, in addition to a 125-kDA protein, a ladder of XPC signals of size between 105- and 125-kDa was detected in both the pathological specimens and LADC cell lines. After CIP treatment, the intensity of the 125-kDa band was reduced and that of the 105-kDa protein increased, indicating that 125-kDa XPC could be phosphorylated. *In vitro*, UV irradiation and exposure to tobacco, nicotine, and cisplatin increased the expression levels of the 125-kDa XPC, suggesting that DNA damage could stabilize XPC via protein phosphorylation. UV irradiation and cisplatin treatment also increased the levels of p53, which occurred before the increase in XPC expression, implying that XPC expression was regulated by p53. Treatment with calphostin C, a pan-PKC inhibitor, reduced UV-induced XPC phosphorylation and the protein levels of 125-kDa XPC, further suggesting that PKC could be the enzyme that catalyzes XPC phosphorylation (21) and that post-translational modification is essential for maintaining XPC stability. Moreover, the tobacco- and nicotine-induced increase in XPC expression was correlated with reduced cisplatin sensitivity in lung cancer cells. In contrast, silencing of XPC expression by using siRNA decreased cisplatin resistance. These results clearly indicate that the expression of XPC is critical for drug resistance in LADC, which then reflected in patient survival. Patients with low XPC expression are more sensitive to cisplatin-based chemotherapy and have a better prognosis. On the other hand, those with high XPC expression are more resistant to chemotherapy and, thus, have a poorer prognosis. By showing that mutations in XPC gene decrease cisplatin-mediated activation of caspase-3, the results from Wang *et al* support our observations and indicate that XPC expression reduces cisplatin-mediated cell death (22). The exact mechanism by which XPC contributes to cisplatin resistance, however, is not yet clear.

It is worth noting that following UV irradiation, XPC and the human homolog of the yeast Rad23 protein B (hHR23B) are promptly imported to the nucleus (23,24). Inside the nucleus, hHR23B increases p53 accumulation, inhibits cell cycle progression, while XPC accelerates DNA repair, and reduces DNA damage-related cell death. The synergistic action of XPC and hHR23B results in cytoresistance to chemotherapeutics and irradiation (23). Our recent report also showed that increase in the amount of nuclear dynamin-related protein 1 (DRP1) accompanied by nuclear accumulation of hHR23A was imperative for the increase of cisplatin resistance (25). Both hHR23A and hHR23B are involved in DNA repair and p53 stabilization. As noted previously, XPC is an important protein for nucleotide excision repair (NER), and in association with hHR23B, XPC binds at DNA damage sites, including UV-induced cyclobutane pyrimidine dimers and chemical-conjugated DNA adducts. The XPC-hHR23B complex recruits XPA, XPB, XPD, RNA polymerase II basal transcription factor b (TFIIH), transcription factor B5 (TFB5), and human replication protein A (RPA) and initiates DNA repair by unwinding the damaged DNA segments. Following the engagement of ERCC1-XPF and XPG, two essential endonucleases, to the multimeric complexes the damaged DNA strand is excised and repaired (6,26). Recently, ERCC1-XPF was shown to be involved in the homologous recombination repair (HRR) of double-stranded breaks induced by interstrand DNA crosslinkage (8,11,26). As noted previously, tobacco smoking introduces intrastrand and interstrand DNA crosslinkage (27-29) as well as oxidative DNA damage (30). Tobacco may similarly induce p53 expression and DNA repair mechanisms. However, it should be noted that other explanations are possible. For instance, cigarette smoking elevates the expression of hepatocyte growth factor (HGF) in LADC cells (4), and HGF down-regulates apoptosis-inducing factor (AIF), thereby increasing cisplatin resistance (5).

Moreover, with the results of the SSH and microarray studies, i.e., that the expressions of XPC, ERCC1, MSH3 and MSH6 mRNA were found to be elevated in patients with advanced disease, considered together with our immunoblotting results clearly indicate that the expression of NER-(7) and mismatch repair-related genes was up-regulated in LADC cells. XPC and ERCC1 could represent a group of NER-associated genes that was correlated with drug resistance and prognosis in NSCLC. Interestingly, deletion of the XPC gene has been shown to increase the possibility of chemically-induced and spontaneous lung cancer (31,32), including benign lung adenoma and LADC. Nonetheless, the frequency at which $XPC^{-/-}$ mice develop LADC (~20%) is similar to that at which $XPC^{+/+}$ B6C3F1 mice that have been forced to inhale cigarette smoke (20.3%, 67/330) develop LADC (33). In $XPC^{-/-}Gadd45^{-/-}$ mice, the incidence of LADC increased up to 60% (26), indicating that double-knockout of DNA repair-related genes indeed elevated the incidence of lung carcinogenesis. However, the life span of $XPC^{-/-}$ or $XPC^{-/-}Gadd45^{-/-}$ mice was not significantly different from that of $XPC^{+/+}$ mice (30). Unfortunately, the efficacy of cisplatin for these spontaneously developed murine lung cancers was not determined.

In conclusion, immunoblotting and immunohistochemical examination revealed abundant expression of the XPC protein in LADC cells. The results of pathological examination suggest that XPC expression is associated with tumor stage and the cigarette smoking habits of patients, which reflect the increased tumor cell growth and poor prognosis. In the *in vitro* experiments with LADC cell lines, tobacco and nicotine increased the XPC protein level and cisplatin resistance in these cells. Moreover, silencing of XPC expression decreased cisplatin resistance. These data suggest that XPC plays a role in drug resistance of LADC cells. However, our study was limited because we used the immunohistochemical method, which only detects the total amount of XPC expressed in LADC cells, but not the degree of XPC phosphorylation. Moreover, our results correspond to a relatively small sample size and need further validation with a study with a large sample size.

Acknowledgments

This study was supported, in part, by the Comprehensive Academic Promotion Projects, Taiwan Department of Education (NCHU 995002 to K.C.C), and, in part, by the Taiwan Department of Health, China Medical University Hospital, Cancer Research of Excellence (DOH99-TD-C-111-005). RNAi for silencing *XPC* gene expression was obtained from the National RNAi Core Facility at the Institute of Molecular Biology/Genomic Research Center, Academia Sinica, Taipei, Taiwan, which is supported by the National Research Program for Genomic Medicine Grants of NSC (NSC 97-3112-B-001-016).

References

1. Annual reports of the Department of Health, the Executive Yuan, Republic of China, 2006.
2. Moran CA and Suster S: Tumors of the lung and pleura. In: Diagnostic Histopathology of Tumors. Fletcher CDM (ed). Churchill Livingstone, London, pp171-208, 2000.
3. Shen H, Spitz MR, Qiao Y, *et al*: Smoking, DNA repair capacity and risk of non-small cell lung cancer. Int J Cancer 107: 84-88, 2003.
4. Chen JT, Lin TS, Chow KC, *et al*: Cigarette smoking induces overexpression of HGF in type II pneumocytes and lung cancer cells. Am J Respir Cell Mol Biol 34: 264-273, 2006.
5. Chen JT, Huang CY, Chiang YY, *et al*: HGF increases cisplatin resistance via down-regulation of AIF in lung cancer cells. Am J Respir Cell Mol Biol 38: 559-565, 2008.
6. Niedernhofer LJ, Odijk H, Budzowska M, *et al*: The structure-specific endonuclease ERCC1-Xpf is required to resolve DNA interstrand cross-link-induced double-strand breaks. Mol Cell Biol 24: 5776-5787, 2004.
7. Olaussen, KA, Dunant A, Fouret P, *et al*: IAL Bio Investigators: DNA repair by ERCC1 in non-small-cell lung cancer and cisplatin-based adjuvant chemotherapy. N Engl J Med 355: 983-991, 2006.
8. de Laat WL, Jaspers NG and Hoeijmakers JH: Molecular mechanism of nucleotide excision repair. Genes Dev 13: 768-785, 1999.
9. Paquet F, Pérez C, Leng M, Lancelot G and Malinge JM: NMR solution structure of a DNA decamer containing an interstrand cross-link of the antitumor drug cis-diamminedichloroplatinum (II). J Biomol Struct Dyn 14: 67-77, 1996.
10. Sancar A, Lindsey-Boltz LA, Unsal-Kaçmaz K and Linn S: Molecular mechanisms of mammalian DNA repair and the DNA damage checkpoints. Annu Rev Biochem 73: 39-85, 2004.
11. Jiricny J: The multifaceted mismatch-repair system. Nat Rev Mol Cell Biol 7: 335-346, 2006.
12. Mountain CF: Revisions in the international system for staging lung cancer. Chest 111: 1710-1717, 1997.
13. Yang GP, Ross DT, Kuang WW, Brown PO and Weigel RJ: Combining SSH and cDNA microarrays for rapid identification of differentially expressed genes. Nucleic Acids Res 27: 1517-1523, 1999.
14. Chavanne F, Broughton BC, Pietra D, *et al*: Mutations in the XPC gene in families with xeroderma pigmentosum and consequences at the cell, protein, and transcript levels. Cancer Res 60: 1974-1982, 2000.
15. Remmele W and Schicketanz KH: Immunohistochemical determination of estrogen and progesterone receptor content in human breast cancer. Computer-assisted image analysis (QIC score) vs. subjective grading (IRS). Pathol Res Pract 189: 862-866, 1993.
16. Kaplan EL and Meier P: Non-parametric estimation from incomplete observations. J Am Stat Assoc 53: 457-481, 1958.
17. Mantel N: Evaluation of survival data and two new rank order statistics arising in its consideration. Cancer Chemother Rep 50: 163-170, 1966.
18. Oz MC, Cosgrove DM III, Badduke BR, *et al*: Controlled clinical trial of a novel hemostatic agent in cardiac surgery. Ann Thorac Surg 69: 1376-1382, 2000.
19. Fautrel A, Andrieux L, Musso O, Boudjema K, Guillouzo A and Langouët S: Overexpression of the two nucleotide excision repair genes ERCC1 and XPC in human hepatocellular carcinoma. J Hepatol 43: 288-293, 2005.
20. Adimoolam S and Ford JM: p53 and DNA damage-inducible expression of the xeroderma pigmentosum group C gene. Proc Natl Acad Sci USA 99: 12985-12990, 2002.
21. Kobayashi E, Nakano H, Morimoto M and Tamaoki T: Calphostin C (UCN-1028C), a novel microbial compound, is a highly potent and specific inhibitor of protein kinase C. Biochem Biophys Res Commun 159: 548-553, 1989.
22. Wang G, Chuang L, Zhang X, *et al*: The initiative role of XPC protein in cisplatin DNA damaging treatment-mediated cell cycle regulation. Nucleic Acids Res 32: 2231-2240, 2004.
23. Kaur M, Pop M, Shi D, Brignone C and Grossman SR: hHR23B is required for genotoxic-specific activation of p53 and apoptosis. Oncogene 26: 1231-1237, 2007.
24. Dominguez-Brauer C, Chen YJ, Brauer PM, Pimkina J and Raychaudhuri P: ARF stimulates XPC to trigger nucleotide excision repair by regulating the repressor complex of E2F4. EMBO Rep 10: 1036-1042, 2009.
25. Chiang YY, Chen SL, Hsiao YT, *et al*: Nuclear expression of dynamin-related protein 1 in lung adenocarcinomas. Mod Pathol 22: 1139-1150, 2009.
26. Wood RD, Mitchell M, Sgouros J and Lindahl T: Human DNA repair genes. Science 291: 1284-1289, 2001.
27. De Silva IU, McHugh PJ, Clingen PH and Hartley JA: Defining the roles of nucleotide excision repair and recombination in the repair of DNA interstrand cross-links in mammalian cells. Mol Cell Biol 20: 7980-7990, 2000.
28. Matsuda T, Kawanishi M, Yagi T, Matsui S and Takebe H: Specific tandem GG to TT base substitutions induced by acetaldehyde are due to intra-strand crosslinks between adjacent guanine bases. Nucleic Acids Res 26: 1769-1774, 1998.
29. Lao Y and Hecht SS: Synthesis and properties of an acetaldehyde-derived oligonucleotide interstrand cross-link. Chem Res Toxicol 18: 711-721, 2005.
30. D'Errico M, Parlanti E, Teson M, *et al*: New functions of XPC in the protection of human skin cells from oxidative damage. EMBO J 25: 4305-4315, 2006.
31. Cheo DL, Burns DK, Meira LB, Houle JF and Friedberg EC: Mutational inactivation of the xeroderma pigmentosum group C gene confers predisposition to 2-acetylaminofluorene-induced liver and lung cancer and to spontaneous testicular cancer in $Trp53^{-/-}$ mice. Cancer Res 59: 771-775, 1999.
32. Hollander MC, Philburn RT, Patterson AD, *et al*: Deletion of XPC leads to lung tumors in mice and is associated with early events in human lung carcinogenesis. Proc Natl Acad Sci USA 102: 13200-13205, 2005.
33. Hutt JA, Vuillemenot BR, Barr EB, *et al*: Life-span inhalation exposure to mainstream cigarette smoke induces lung cancer in B6C3F1 mice through genetic and epigenetic pathways. Carcinogenesis 26: 1999-2009, 2005.